JACS
JOURNAL OF THE AMERICAN CHEMICAL SOCIETY
Article
pubs.acs.org/JACS

Sonogashira Cross-Coupling and Homocoupling on a Silver Surface: Chlorobenzene and Phenylacetylene on Ag(100)

Carlos Sanchez-Sanchez,[†,‡] Noe Orozco,[†] Juan P. Holgado,[†] Simon K. Beaumont,[§] Georgios Kyriakou,[∥] David J. Watson,[⊥] Agustin R. Gonzalez-Elipe,[†] Leticia Feria,[#,¶] Javier Fernández Sanz,[¶] and Richard M. Lambert*[,†,▲]

[†]Instituto de Ciencia de Materiales de Sevilla (CSIC), Americo Vespucio 49, 41092 Seville, Spain
[‡]EMPA, Swiss Federal Laboratories for Materials Science and Technology, Überlandstrasse 129, 8600 Dübendorf, Switzerland
[§]Department of Chemistry, Durham University, South Road, Durham DH1 3LE, United Kingdom
[∥]Department of Chemistry, University of Hull, Hull HU6 7RX, United Kingdom
[⊥]Department of Chemistry, University of Surrey, Guildford GU2 7XH, United Kingdom
[#]Departamento de Química, Universidad Técnica Particular de Loja, P.O. Box 11-01-608, Loja, Ecuador
[¶]Departamento de Química Física, Facultad de Química, Universidad de Sevilla, E-41012 Sevilla, Spain
[▲]Chemistry Department, Cambridge University, Cambridge CB2 1EW, United Kingdom

Supporting Information

ABSTRACT: Scanning tunneling microscopy, temperature-programmed reaction, near-edge X-ray absorption fine structure spectroscopy, and density functional theory calculations were used to study the adsorption and reactions of phenylacetylene and chlorobenzene on Ag(100). In the absence of solvent molecules and additives, these molecules underwent homocoupling and Sonogashira cross-coupling in an unambiguously heterogeneous mode. Of particular interest is the use of silver, previously unexplored, and chlorobenzene—normally regarded as relatively inert in such reactions. Both molecules adopt an essentially flat-lying conformation for which the observed and calculated adsorption energies are in reasonable agreement. Their magnitudes indicate that in both cases adsorption is predominantly due to dispersion forces for which interaction nevertheless leads to chemical activation and reaction. Both adsorbates exhibited pronounced island formation, thought to limit chemical activity under the conditions used and posited to occur at island boundaries, as was indeed observed in the case of phenylacetylene. The implications of these findings for the development of practical catalytic systems are considered.

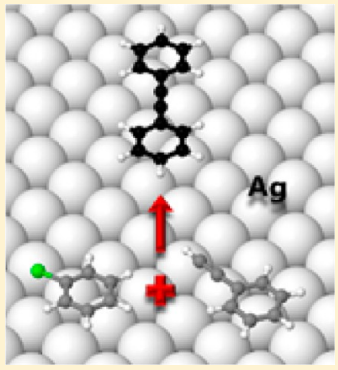

INTRODUCTION

Metal-catalyzed Sonogashira coupling reactions that lead to the formation of new C−C bonds are of strategic importance in synthetic organic chemistry. They provide a powerful and flexible method for systematically and efficiently constructing complex molecular architectures from suitably tailored building blocks and are now the most important method for preparing arylalkynes and conjugated enynes, which are key precursors in the synthesis of natural products, pharmaceuticals, and organic molecular materials.[1] Palladium species constitute by far the most commonly used catalysts, usually applied in the form of soluble complexes of the metal. However, opinion remains strongly divided in regard to the identity of the catalytically active species: are they soluble metal complexes or the surfaces of metallic nanoparticles that are present in equilibrium with such complexes? In a solution environment, unambiguous resolution of this question is far from trivial.[2]

Recently, gold nanoparticles in a solution were used to catalyze the cross-coupling of iodobenzene with phenylacetylene—a prototypical and very widely studied example of Sonogashira coupling.[3,4]

In this case, evidence was presented in favor of heterogeneous as opposed to homogeneous catalysis as the key process involved.[5] The demonstration of this reaction on the Au(111) surface[6] and, more recently, on the Au(100) surface[7] *in a vacuum environment* provides compelling support for the view that gold-catalyzed Sonogashira coupling does indeed take place at the metal surface.

Although much work has been carried out on Sonogashira coupling of a wide range of terminal alkynes with aryl iodides, the use of aryl chlorides has been relatively neglected, despite the fact that they are more widely available and less costly than the corresponding iodides (and bromides). Aryl chloride-based Sonogashira coupling is relatively difficult, presumably due to the substantially greater strength of the C−Cl bond (D°_{298K}(Cl−CH_3) = 350 kJ/mol) compared to the C−I bond (D°_{298K}(I−

Received: November 10, 2014
Published: December 22, 2014

DOI: 10.1021/ja5115584
J. Am. Chem. Soc. 2015, 137, 940−947

CH_3) = 239 kJ/mol).[8,9] Success has been achieved in some cases, for example, by Lee et al., who used pyridylazetidine-based Pd(II) complexes as homogeneous catalysts to couple phenylacetylene with various aryl chlorides and bromides,[10] but reports of heterogeneously catalyzed Sonogashira coupling with aryl chlorides are very rare and typically focus only on highly activated keto- and aldehyde-substituted aryl chlorides.[11] Surface-tethered organometallic Pd-based catalysts have been found to catalyze the reaction with aryl chloride substrates,[12] but as ever, the use of immobilized homogeneous complexes brings the drawback of inevitable leaching of the active monatomic metal center, which must be held by relatively labile coordinate bonds in order for catalysis to occur.[13] The present study is focused on use of chlorobenzene, a simple unactivated aryl chloride that is representative of the reactants that it would be desirable to employ in routine synthetic transformations.

Given the high cost of palladium and gold and their complexes, the successful application of a relatively inexpensive metal such as silver as a simple heterogeneous catalyst for Sonogashira coupling of aryl chlorides with terminal alkynes would address simultaneously the issues of cost (Ag ($31/oz), Pd ($644/oz))[14] and recyclability, both of which are important in regard to potential large-scale use. Here we report a study of the Sonogashira coupling of phenylacetylene (PA) with chlorobenzene (ClBz) on the Ag(100) surface under vacuum by means of scanning tunneling microscopy (STM), temperature-programmed reaction (TPR), and near-edge X-ray absorption fine structure (NEXAFS) spectroscopy, supported by density functional theory (DFT) calculations. The reaction does indeed occur and clearly is a strictly heterogeneous process. Both reactants show a pronounced tendency to form islands on extended terraces, which is thought to account for the relatively low reaction yields under conditions of TPR. The insight acquired here should enable rational design of practical, cheap, and widely applicable silver-based heterogeneous catalysts for this important reaction.

METHODOLOGY

Experimental Methods. STM data were acquired with an Omicron VT-STM instrument previously described.[7] Temperature-programmed desorption (TPD) and TPR measurements were carried out in a stainless steel ultrahigh vacuum chamber of conventional design operated at a base pressure of 2×10^{-10} mbar. It was equipped with a VG 300 quadrupole mass spectrometer for residual gas analysis and temperature-programmed desorption, a 3 grid retarding field analyzer with integral electron gun and fluorescent screen for LEED/AES, and an ion gun for Ar^+ sputtering. The resistively heated Ag(100) single crystal was mounted on a sample holder by means of Ta clips and attached to the *XYZθ* manipulator equipped with liquid nitrogen cooling, enabling sample temperatures from ∼120 to 1300 K. TPR data were taken using a linear temperature ramp (3 K/s) delivered by a programmed power supply. Crystal temperature was monitored via a K-type thermocouple retained on the top edge of the sample with a Ta clip. The distance from the crystal front face to the collimating entrance orifice of the mass spectrometer was <10 mm: control experiments confirmed that the detected desorbing species originated entirely from the front face of the sample. In the STM, temperature was recorded somewhat indirectly by means of a Si diode that was in good thermal contact with a cooled heat sink, whereas both it and the sample were in less good contact with the proprietary Omicron PBN heater. As a consequence, equilibrated sample temperatures attained on cooling were accurate, but temperatures recorded during short annealing steps were subject to an unknown (likely substantial) error due to thermal lag effects. These temperatures should therefore be interpreted only comparatively. Precise measurement of sample temperature in the STM was unimportant when following behavior of adsorbates during stepwise annealing. Estimated adsorbate exposures are specified in Langmuirs (1L = 1.33×10^{-6} mbar·s), derived from the total pressure during dosing and partial pressures observed simultaneously by quadrupole mass spectrometry.

NEXAFS data were acquired on the SuperESCA beamline at the ELETTRA synchrotron radiation facility in Trieste, Italy. Relevant experimental details are provided elsewhere.[15−17] The data were processed by standard methodology,[18] with the photon energy being corrected to the C K-edge dip in the monochromator output.[19] Energy calibration and intensity normalization were carried out following established procedures,[19] and low-frequency noise in the spectral data (≪0.5 eV) was reduced by use of a three-point low-pass binomial filter.[20] During the NEXAFS experiments, the Ag(100) sample was cleaned by cycles of Ar^+ bombardment (Ar (99.999%, Messer) pressure 3×10^{-6} mbar ≈ 6 μA) at room temperature (20 min), 700 K (15 min), and again at room temperature (15 min), followed by annealing in vacuum at 700 K (15 min). Cleanliness was confirmed by both a sharp (1 × 1) LEED pattern and the absence of contamination detectable by XPS. The organic adsorbates (Sigma-Aldrich) were dosed by backfilling the vacuum chamber with an accurately measured pressure of the vapor after purification by repeated freeze/pump/thaw cycles. Spectra were collected using a single-pass 32-channel concentric hemispherical electron analyzer. The angle between the analyzer entrance lens and the incoming photon beam was 70° in the horizontal plane, and the degree of linear polarization of the photons was 0.99. Repetition of one NEXAFS spectrum during each set acquired showed that there were no detectable beam damage effects on the adsorbed layer during the acquisition of NEXAFS data. Quoted coverages are based on estimation of the monolayer point (one monolayer = 1 ML) from a shift in C 1s binding energy in the XPS.

DFT Calculations. The theoretical calculations of ClBz/Ag(100) and PA/Ag(100) models were performed within the DFT framework. The Perdew, Burke, and Ernzerhof (PBE) functional was used for the exchange-correlation potential.[21] The effect of the core electrons on the valence states was represented with the projector-augmented wave approach,[22] as implemented in the Vienna ab initio simulation package (VASP).[23,24] We treated explicitly the H (1s), C (2s, 2p), Ag (4d, 5s), and Cl (3s, 3p) electrons as valence electrons, and their wave functions were expanded in a plane-wave basis set with a cutoff energy of 500 eV for the kinetic energy.

Long-range van der Waals (vdW) forces play a key role in describing the interaction between organic molecules and metallic surfaces, and the way to introduce them into the DFT scheme still is being debated. For benzene, the 111 adsorption energy on coinage metals increases by about 0.7 eV when the vdW correction is included,[25] that is, on the order of the interaction energy itself, which causes that with or without long-range forces to make the system bound or unbound. In the present work, to account for the contributions of vdW forces, a nonlocal exchange-correlation functional was used, in particular, the optimized Becke86b (optB86b-vdW) functional. The vdW DFT calculations were carried out self-consistently using the implementation in VASP code by Klimes et al.,[26] employing the algorithm of Román-Pérez and Soler.[27] This functional has been shown to adequately render the surface−adsorbate distances in related systems, while the adsorption energy is overestimated by 10% in the case of benzene supported on the Cu(111) surface.[25,28,29]

The Ag(100) surface was modeled by a (8 × 4) supercell containing 128 atoms in four layers. The supercell is repeated periodically into the three directions with a vacuum region of 15 Å between the slabs. This model is large enough to accommodate a single adsorbed species while avoiding lateral interactions. In the optimizations, the two outermost layers of one side of the slab were completely allowed to relax while the other two layers were kept frozen. All the calculations were performed at the Γ point of the Brillouin zone.

DOI: 10.1021/ja5115584
J. Am. Chem. Soc. 2015, 137, 940−947

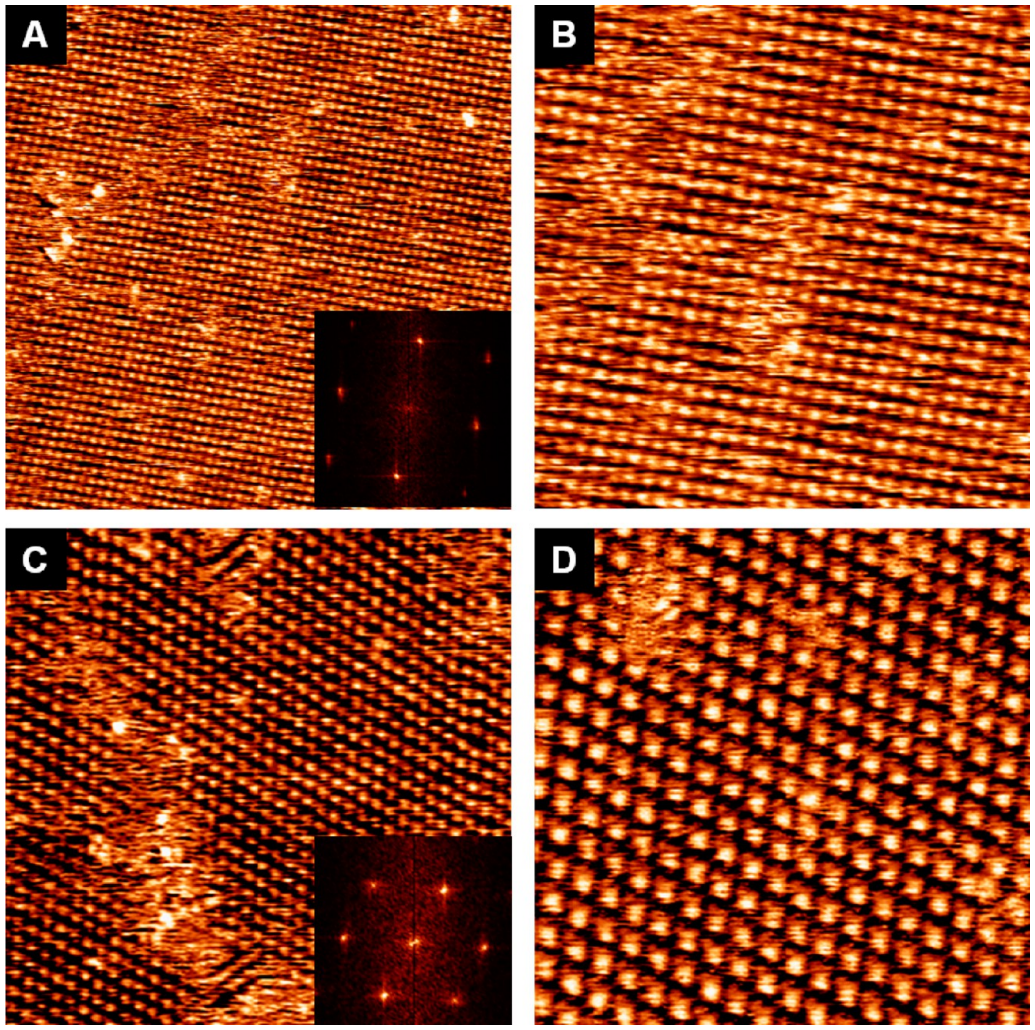

Figure 1. STM images of two different chlorobenzene phases coexisting on the Ag(100) surface after gentle annealing (Si diode temperature = 240 K). Exposure: 2L. (A) STM image of the rectangular phase. Inset: Fast Fourier transform of the STM image. STM parameters: (75 nm × 75 nm) I = 0.65 nA, V = 1.76 V. (B) Higher magnification image of the rectangular phase. Each bright feature corresponds to a ClBz molecule. STM parameters: (40.0 nm × 40.0 nm) I = 0.65 nA, V = 1.76 V. (C) STM image of the hexagonal phase. Inset: Fast Fourier transform of the STM image. STM parameters: (50 nm × 50 nm) I = 0.65 nA, V = 1.76 V. (D) Higher magnification image of the hexagonal structure. Each bright feature corresponds to a ClBz molecule. STM parameters: (25 nm × 25 nm) I = 0.44 nA, V = 1.94 V.

■ RESULTS AND DISCUSSION

Both experiment and theory show that phenylacetylene and chlorobenzene lie almost flat on the Ag(100) surface and are essentially physisorbed. Despite this relatively weak interaction with the underlying silver, both species undergo homocoupling to yield the corresponding gaseous products. They also cross-couple to form diphenylacetylene, an important process never previously reported as being catalyzed by silver. Noteworthy too is the use of chlorobenzene, a relatively inert halobenzene, far less investigated than the much more reactive bromine and iodine analogues. All the chemistry occurs in a strictly heterogeneous mode, an observation of relevance to the continuing debate concerning the question of homogeneous versus heterogeneous catalysis in such organic reactions. The reactants spontaneously form islands, and in the case of chlorobenzene, the initiation of the chemical reaction at island boundaries was imaged. In the case of Sonogashira cross-coupling, it is presumed that the two types of island would have to be proximate. This behavior is thought to account for the low product yields observed under our "one-shot" conditions. In light of these findings, strategies for achieving high conversions under conditions of steady-state catalytic reactions are proposed.

STM and NEXAFS Spectroscopy. *STM.* Chlorobenzene adsorption at 120 K followed by gentle annealing (~240 K) produced the image shown in Figure 1A and in more detail in Figure 1B (rectangular structure), along with the corresponding Fourier transform. The rectangular phase coexisted with an equally well-ordered hexagonal phase (Figure 1C,D), with the two being separated by domain boundaries (Figure 2) and corresponding to equal coverages. The hexagonal phase may be generated from a perfect rectangular phase by displacing alternate rows of the former by half a lattice parameter along the ⟨001⟩ direction.

The observed unit cell of the rectangular phase was ~1.65 nm × 1.40 nm, where distortion from four-fold symmetry may be rationalized in terms of maximizing favorable dipole−dipole interactions, as illustrated in Figure 3A (a perfect 5 × 5 overlayer would correspond to 1.44 nm × 1.44 nm); Figure 3B similarly illustrates a plausible structure for the (undistorted) hexagonal phase.

DOI: 10.1021/ja5115584
J. Am. Chem. Soc. 2015, 137, 940−947

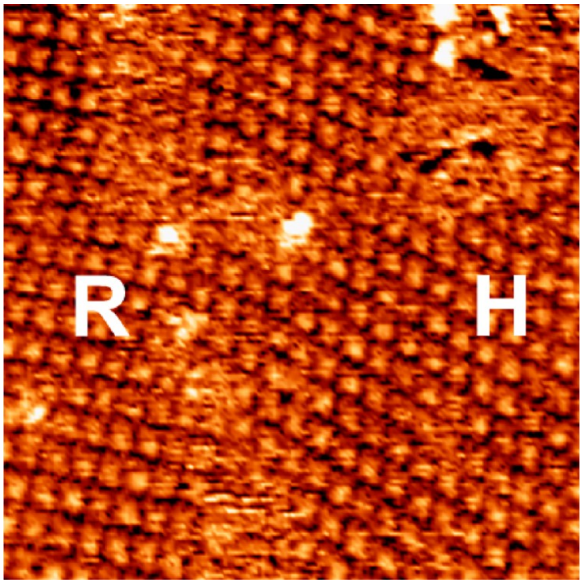

Figure 2. STM image of ClBz on Ag(100) after gentle annealing (Si diode temperature = 240 K), showing coexistence of rectangular (R) and hexagonal (H) phases. STM parameters: (30 nm × 30 nm) I = 0.27 nA, V = 1.94 V.

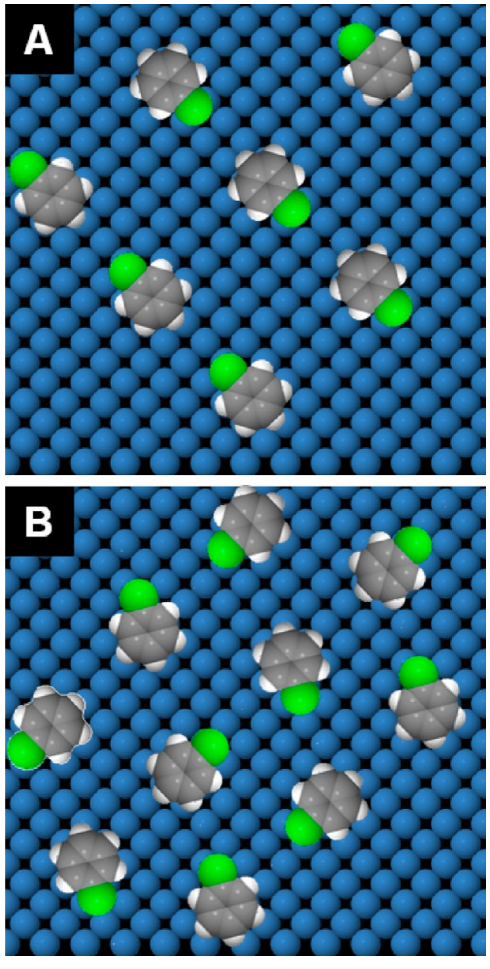

Figure 3. Schematic representation of plausible ClBz structures. Molecules have been represented by their vdW radii: (A) rectangular phase; (B) hexagonal phase. Color code: green (chlorine), gray (carbon), white (hydrogen), and blue (silver).

The proposed structures take account of the large dipole moment of the free chlorobenzene molecule (1.6 D) and the fact that the in-plane molecular dipole is likely to be substantially amplified on Ag(100) by adsorbate → metal charge transfer.[30] Given the coexistence of these two island-forming phases, no particular registry between the molecular overlayer and the underlying surface has been chosen, which is also consistent with the DFT results (see below).

In addition to the hexagonal and rectangular phases of adsorbed chlorobenzene molecules, in a few areas of the sample, the onset/appearance of elongated features could be seen (Figure 4A), the most likely explanation for which is formation of rows of biphenyl molecules. The inter-row separation is 0.54 nm, sufficient to accommodate the width of biphenyl. Heating to higher temperature resulted in more

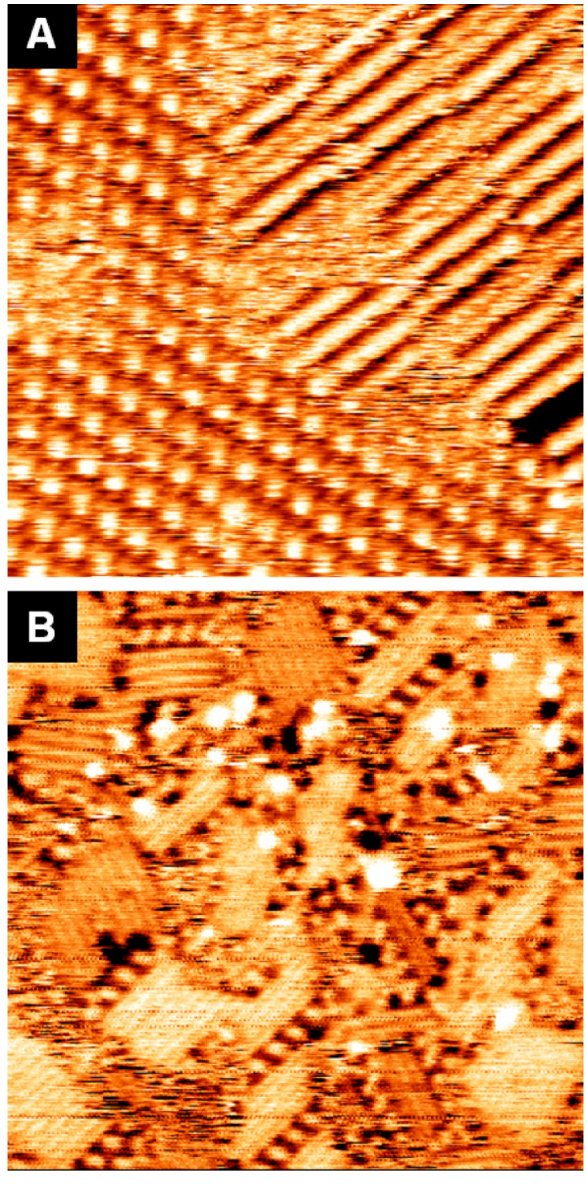

Figure 4. STM images showing progressive formation of biphenyl with increasing temperature: (A) (25.0 nm × 25.0 nm) I = 0.44 nA, V = 2.1 V, following further annealing (Si diode temperature = 240 K); (B) (25.0 nm × 25.0 nm) I = 0.38 nA, V = 2.1 V, following annealing to higher temperature (Si diode temperature = 295 K).

DOI: 10.1021/ja5115584
J. Am. Chem. Soc. 2015, 137, 940–947

extensive reaction, as shown in Figure 4B, where now the product molecules are predominant.

A typical image resulting from exposure of the clean Ag(100) surface to phenylacetylene at 120 K followed by annealing (~200 K) for 10 min is shown in Figure 5A. Well-ordered

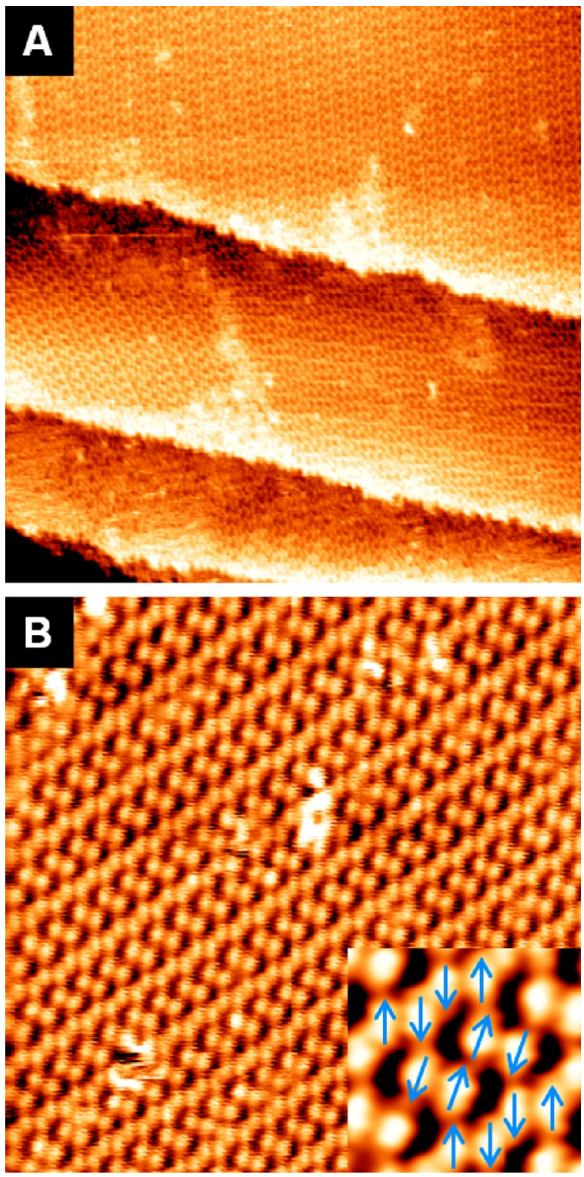

Figure 5. Phenylacetylene island growth on Ag(100). See text. Exposure: 4 L. (A) (75 nm × 75 nm) I = 0.31 nA, V = 1.89 V; (B) (25 nm × 25 nm) I = 0.40 nA, V = 2.31 V. Inset: Magnified image with a superimposed dipole model illustrated with blue arrows.

adsorbate islands were formed, with no preferred orientation relative to the underlying metal surface mesh or step edges, indicating that adsorbate−adsorbate attractive interactions dominated. Note especially the two domains on the second step down oriented at ~120° with respect to each other. Figure 5B shows the overlayer structure in more detail. The inset to Figure 5B illustrates a possible molecular arrangement that takes into account the dipole−dipole interactions, indicated by arrows, keeping in mind that the molecules in the long rows are alternately displaced up and down with respect to the row direction.

NEXAFS Spectroscopy of Individual Reactants on Ag(100). NEXAFS measurements were carried out on ClBz and PA separately adsorbed in a similar manner to the STM images above (Figures 1, 2, 4, and 5). As will be shown, both cases provide support for the molecules being absorbed with phenyl rings almost flat, in agreement with the above structural models and the conformations seen by STM. Figure 6 shows C K-edge NEXAFS spectra of 1.0 ML of PA on Ag(100) at 170 K recorded at five photon incidence angles (θ, defined relative to the surface plane). Prominent resonances due to aromatic C 1s → π^* and acetylenic C 1s → π^* are apparent, in addition to a broad higher energy feature due to C 1s → σ^* transitions, as indicated in Figure 6.

The C 1s → π^* resonances at 284.9 and 285.7 eV are crucial for estimating the orientation of PA on Ag(100): Figure 6B shows the same spectra expanded about this region, and it can be seen that opposing q dependences exist for the C 1s → π_{Ar}^* (aromatic ring) and C 1s → π_{Ac}^* (alkyne group) transitions. This behavior can be understood in terms of a flat-lying molecule in which the aromatic ring C 1s → π_{Ar}^* transition is to an orbital of maximum amplitude out-of-plane of the molecule and the surface. (Similarly, the acetylenic resonance with the opposite q dependence is due to the component of the C≡C bond that is not conjugated to the ring and so is of maximal amplitude in-plane with the molecule and the surface.) A detailed discussion of the assignment of phenylacetylene resonances is provided in our previous work[6] but is not required for the present analysis. Figure 6C shows the angular dependence of the C 1s → π_{Ar}^* resonance used to determine the orientation of the molecules with respect to the surface by overlying the normalized intensities with a series of theoretical curves,[31] with the least-squares best fit yielding a tilt angle of α = 28° with an uncertainty of 5° for the orientation of the phenyl group with respect to the surface; that is, the molecule lies almost flat to the surface.

Similarly, Figure 7A shows C K-edge NEXAFS spectra for 1.0 ML of ClBz at 170 K acquired at five photon incidence angles. The first two resonances at 284.8 and 286.1 eV are assigned to C 1s → π^* transitions, split by 1.3 eV into two components due to the presence of the chlorine heteroatom (either as a result of the reduction in symmetry from D_{6h} to C_{2v} or a core level shift in the C 1s level as discussed for halobenzene adsorption on other metal surfaces).[32] This is more clearly apparent in Figure 7B. Furthermore, in Figure 7A at 287.8 eV, a feature with the opposite q dependence is seen, most likely attributable to σ_{C-Cl}^*.[32] In combination, these features provide strong evidence that adsorption of ClBz and heating to 170 K do not result in scission of the C−Cl bond, in good accord with the STM data that show intact molecules following adsorption and mild annealing.

The angular dependence of the C 1s → π_1^* resonance at 284.8 eV was used to calculate the orientation of ClBz with respect to the surface as before, and the results are shown in Figure 7C: ClBz also adsorbs relatively flat on the surface, with tilt angle α = 26° (uncertainty of 5°), consistent with the structural models outlined above.

Calculated Adsorption Energies of Phenylacetylene and Chlorobenzene. DFT calculations were carried out as described above to obtain geometry-optimized adsorption energies for both molecules for five different high symmetry sites. It was found that in both cases the adsorption energy was relatively insensitive to the site symmetry between 0.81 and 1.08 eV for phenylacetylene and between 0.71 and 0.94 eV for

DOI: 10.1021/ja5115584
J. Am. Chem. Soc. 2015, 137, 940−947

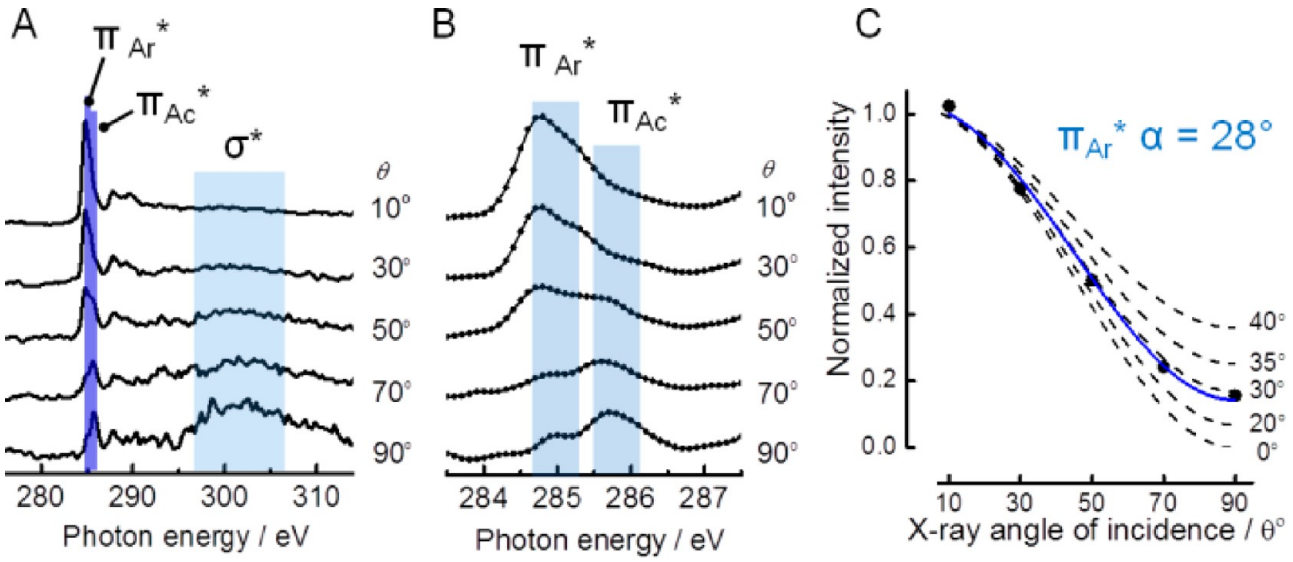

Figure 6. (A) C K-edge NEXAFS spectra acquired at five angles of photon incidence θ for a ~1.0 ML coverage of PA on Ag(100) at 170 K. (B) Leading π^* resonances, expanded scale (Ar = aromatic; Ac = acetylenic). (C) Curve-fitting analysis of q dependence of π^* resonance A to estimate the phenyl ring tilt angle, α.

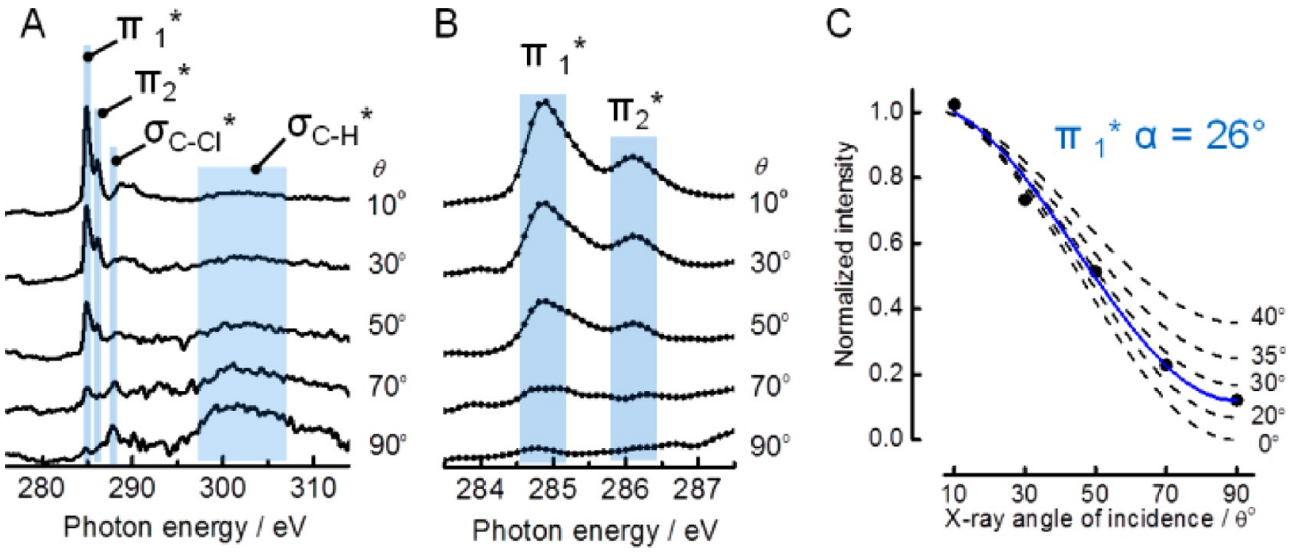

Figure 7. (A) C K-edge NEXAFS spectra acquired at five photon incidence angles θ for a ~1.0 ML coverage of ClBz on Ag(100). (B) Principal π^* resonances expanded scale. (C) Curve-fitting analysis of the photon angle dependence of π_1^* resonance to estimate the corresponding phenyl ring tilt angle, α.

chlorobenzene. The most favorable configurations corresponded to almost flat-lying molecules in hollow sites and are illustrated in the Supporting Information (Figure S1). These structures and the associated energies indicate that both molecules are essentially physisorbed as a result of the dispersive interaction between the aromatic rings and the silver surface. In the case of phenylacetylene, a small distortion of the terminal carbon atom was observed in the optimized structure, consistent with the somewhat larger calculated interaction energy for this case. The importance of the van der Waals forces acting in these systems may be estimated within DFT by simply switching off the long-range interaction term. Such DFT-PBE calculations yield adsorption energies of only 0.01(5) and 0.09 eV for chlorobenzene and phenylacetylene, respectively, clearly demonstrating the dominant role of the van der Waals interactions in both cases. Hence the DFT results indicate that the adsorption of both molecules is principally due to the dispersive interaction between the aromatic ring and the metal surface.

Homocoupling and Sonogashira Cross-Coupling of Chlorobenzene and Phenylacetylene. *Temperature-Programmed Desorption and Reaction.* Figure 8A shows typical thermal desorption data for phenylacetylene from the clean surface following exposure at 105 K (see figure caption for exposure details); the inset shows the corresponding desorption of reactively formed diphenyldiacetylene. Figure 8B shows analogous results for chlorobenzene and its homocoupling product, biphenyl. In each case, homocoupling of pure phenylacetylene, homocoupling of pure chlorobenzene, and reaction of coadsorbed phenylacetylene and chlorobenzene, desorption was dominant and the extent of conversion of reactants to products was on the order of a few percent. In the

DOI: 10.1021/ja5115584
J. Am. Chem. Soc. 2015, 137, 940−947

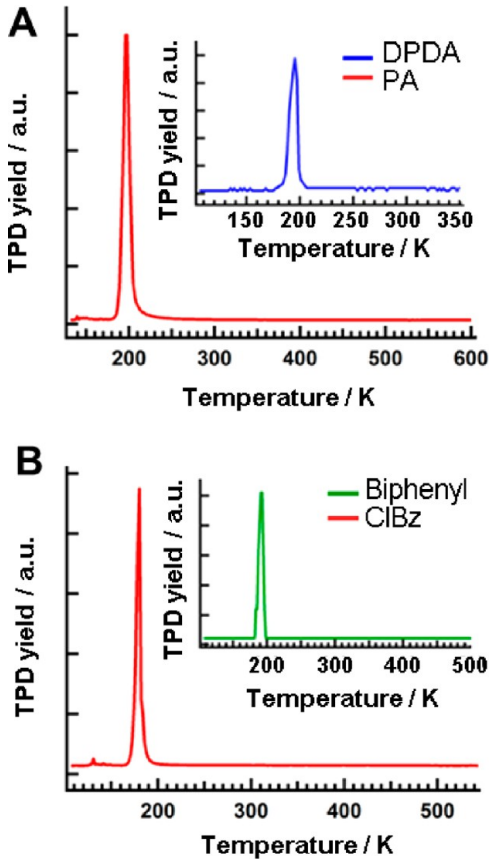

Figure 8. TPD and TPR spectra for both reactants. (A) TPD spectrum of PA adsorption on clean Ag(100) at 105 K. Exposure: 0.6L. Inset: TPR spectrum of the reaction product DPDA. Exposure: 15L. (B) TPD spectrum of ClBz adsorbed on a clean Ag(100) surface at 105 K. Exposure: 0.2L. Inset: TPR spectrum of the reaction product BP. Exposure: 6L. All spectra were filtered to reduce noise signal.

latter case, as is evident from Figure 9, the three possible products were formed in comparable amounts.

The adsorption energies of the reactants, estimated from peak temperatures and based on either half-order (desorption from adsorbate islands) or first-order desorption kinetics with a prefactor of 10^{13} s^{-1}, were very similar, namely, ~0.6 eV. The level of agreement with the DFT estimates is reasonable,

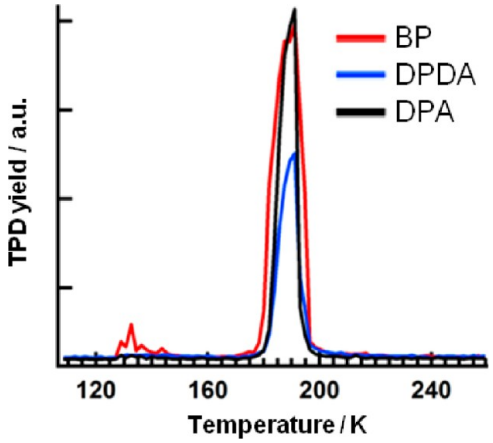

Figure 9. TPR spectra for the reaction products. Both homocoupling and Sonogashira are observed. Exposure: 3L.

bearing in mind that the calculated values are thermally uncorrected and the experimental estimate is subject to some uncertainty. Thus, experiment and theory show that both reactants lay almost flat on the metal surface to which they were relatively weakly bound by dispersion forces, where the interaction was nevertheless sufficient to induce coupling reactions that do not occur otherwise.

It thus appears that, in the complete absence of solvent molecules and any additives, a silver surface can induce Sonogashira coupling. We have no direct evidence concerning the reaction pathway followed by these surface reactions. The widely accepted mechanism for Sonogashira coupling in solution homogeneously catalyzed by Pd/Cu involves Ar−Cl bond cleavage via oxidative addition to a palladium center and corresponding alkyne−H bond cleavage by Cu, followed by combination of the resulting fragments. In the present case, it therefore seems reasonable to suppose that the silver surface similarly activates both reactants toward bond cleavage, followed by coupling of the reaction intermediates and immediate desorption of the product—consistent with the inability to observe such intermediates by STM and NEXAFS spectroscopy.

To our knowledge, this is the first demonstration that metallic Ag is active toward Sonogashira chemistry and indeed that it works with a simple aryl chloride—which is of particular interest for the reasons given in the Introduction. The limited yields of all reaction products under conditions of temperature-programmed reaction, by definition a "one-shot" procedure, may be rationalized as follows. Both reactants exhibit very pronounced island-forming propensities, and because reaction occurs only at island boundaries, under our conditions, most molecules desorb before they can react. With respect to possible practical implementation, under steady-state conditions and in the presence of a solvent, one may anticipate that substantial conversion over time should be possible. Moreover, by judicious use of either small metal nanoparticles or bimetallic materials as a strategy for preventing the growth of large islands, it might be possible to enhance further the intrinsic catalytic activity.

■ CONCLUSIONS

Experiment and theory show that chlorobenzene and phenylacetylene are relatively weakly adsorbed in an essentially flat-lying conformation on the Ag(100) surface, principally the result of dispersive forces. Nevertheless, these molecules undergo both homocoupling and Sonogashira cross-coupling—the first demonstration of catalysis of such reactions by metallic silver and in a mode that is unambiguously heterogeneous. Overall activity is constrained by adsorbate island formation, and the present findings signpost possible approaches for the development of practical catalysts in which such island formation may be inhibited by use of small nanoparticles and/or bimetallic materials, effective for coupling reactions of relatively inactive aryl halides.

■ ASSOCIATED CONTENT

Supporting Information

DFT-optimized structures for chlorobenzene and phenylacetylene adsorbed on the Ag(100) surface. This material is available free of charge via the Internet at http://pubs.acs.org.

DOI: 10.1021/ja5115584
J. Am. Chem. Soc. 2015, 137, 940−947

AUTHOR INFORMATION

Corresponding Author

rml1@cam.ac.uk

Notes

The authors declare no competing financial interest.

ACKNOWLEDGMENTS

This work was supported by the Spanish Ministry of Economy and Competitiveness under projects MAT2013-42900-P, MAT2013-40852-R, MAT2012-31526, and CSD2008-0023. L.F. acknowledges Fellowship support by Prometeo-Project and SENESCyT (Ecuador). S.K.B. acknowledges the award of an Addison Wheeler Fellowship by Durham University and support from The Leverhulme Trust (U.K.). G.K. acknowledges the award of a travel grant from the Royal Society of Chemistry. The authors thank Silvano Lizzit for his assistance during the synchrotron experiments.

REFERENCES

(1) Chinchilla, R.; Najera, C. *Chem. Rev.* **2007**, *107*, 874−922.
(2) Beaumont, S. K. *J. Chem. Technol. Biotechnol.* **2012**, *87*, 595−600.
(3) Gonzalez-Arellano, C.; Abad, A.; Corma, A.; Garcia, H.; Iglesias, M.; Sanchez, F. *Angew. Chem., Int. Ed.* **2007**, *46*, 1536−1538.
(4) Beaumont, S. K.; Kyriakou, G.; Lambert, R. M. *J. Am. Chem. Soc.* **2010**, *132*, 12246−12248. Kanuru, V. K.; Humphrey, S. M.; Kyffin, J. M. W.; Jefferson, D. A.; Burton, J. W.; Armbruster, M.; Lambert, R. M. *Dalton Trans.* **2009**, 7602−7605.
(5) Kyriakou, G.; Beaumont, S. K.; Humphrey, S. M.; Antonetti, C.; Lambert, R. M. *ChemCatChem* **2010**, *2*, 1444−1449.
(6) Kanuru, V. K.; Kyriakou, G.; Beaumont, S. K.; Papageorgiou, A. C.; Watson, D. J.; Lambert, R. M. *J. Am. Chem. Soc.* **2010**, *132*, 8081−8086.
(7) Sánchez-Sánchez, C.; Yubero, F.; González-Elipe, A. R.; Feria, L.; Fernández Sanz, J.; Lambert, R. M. *J. Phys. Chem. C* **2014**, *118*, 11677−11684.
(8) Bedford, R. B.; Cazin, C. S. J.; Holder, D. *Coord. Chem. Rev.* **2004**, *248*, 2283−2321.
(9) *CRC Handbook of Chemistry and Physics*, 88th ed.; Taylor and Francis Group: Boca Raton, FL, 2007.
(10) Lee, D.-H.; Lee, Y. H.; Harrowfield, J. M.; Lee, I. M.; Lee, H. I.; Lim, W. T.; Kim, Y.; Jin, M.-J. *Tetrahedron* **2009**, *65*, 1630−1634.
(11) Cwik, A.; Hell, Z.; Figueras, F. *Tetrahedron Lett.* **2006**, *47*, 3023−3026.
(12) Jin, M.-J.; Lee, D.-H. *Angew. Chem., Int. Ed.* **2010**, *49*, 1119−1122.
(13) Dioos, B. M.; Vankelecom, I. F.; Jacobs, P. *Adv. Synth. Catal.* **2006**, *348*, 1413. Jones, C. *Top. Catal.* **2010**, *53*, 942−952.
(14) London Bullion Market Association. *Forecast 2013*.
(15) Cropley, R. L.; Williams, F. J.; Urquhart, A. J.; Vaughan, O. P. H.; Tikhov, M. S.; Lambert, R. M. *J. Am. Chem. Soc.* **2005**, *127*, 6069−6076.
(16) Brandt, K.; Chiu, M. E.; Watson, D. J.; Tikhov, M. S.; Lambert, R. M. *J. Am. Chem. Soc.* **2009**, *131*, 17286−17290.
(17) Beaumont, S. K.; Kyriakou, G.; Watson, D. J.; Vaughan, O. P. H.; Papageorgiou, A. C.; Lambert, R. M. *J. Phys. Chem. C* **2010**, *114*, 15075−15077.
(18) Stöhr, J.; Jaeger, R. *Phys. Rev. B* **1982**, *26*, 4111−4131.
(19) Schöll, A.; Zou, Y.; Schmidt, T.; Fink, R.; Umbach, E. *J. Electron Spectrosc. Relat. Phenom.* **2003**, *129*, 1−8.
(20) Marchand, P.; Marmet, L. *Rev. Sci. Instrum.* **1983**, *54*, 1034−1041.
(21) Perdew, J. P.; Burke, K.; Ernzerhof, M. *Phys. Rev. Lett.* **1996**, *77*, 3865−3868.
(22) Kresse, G.; Joubert, J. *Phys. Rev. B* **1999**, *59*, 1758−1775.
(23) Kresse, G.; Hafner, J. *Phys. Rev. B* **1993**, *47*, 558−561.
(24) Kresse, G.; Furthmuller, J. *Comput. Mater. Sci.* **1996**, *6*, 15−50.
(25) Yildirim, H.; Greber, T.; Kara, A. *J. Phys. Chem. C* **2013**, *117*, 20572−20583.
(26) Klimes, J.; Bowler, D. R.; Michaelides, A. *Phys. Rev. B* **2011**, *83*, 195131.
(27) Román-Pérez, G.; Soler, J. M. *Phys. Rev. Lett.* **2009**, *103*, 096102.
(28) Reckien, W.; Eggers, M.; Bredow, T. *Beilstein J. Org. Chem.* **2014**, *10*, 1775−1784.
(29) Carrasco, J.; Liu, W.; Michaelides, A.; Tkatchenko, A. *J. Chem. Phys.* **2014**, *140*, 084704.
(30) Vaughan, O. P. H.; Alavi, A.; Williams, F. J.; Lambert, R. M. *Angew. Chem., Int. Ed.* **2008**, *47*, 2422−2426.
(31) Stöhr, J.; Outka, D. A. *Phys. Rev. B* **1987**, *36*, 7891−7905.
(32) Yang, M. X.; Xi, M.; Yuan, H. J.; Bent, B. E.; Stevens, P.; White, J. M. *Surf. Sci.* **1995**, *341*, 9−18.

DOI: 10.1021/ja5115584
J. Am. Chem. Soc. 2015, 137, 940−947